Available online at www.sciencedirect.com

SCIENCE DIRECT®

Microelectronic Engineering 73–74 (2004) 59–62

MICROELECTRONIC ENGINEERING

www.elsevier.com/locate/mee

Design of a tri-layer bottom anti-reflective coating for KrF, ArF and F_2 lithographies

W.C. Cheng [a], F.D. Lai [b], H.M. Huang [b], Lon A. Wang [a,*]

[a] *Department of Electrical Engineering and Graduate Institute of Electro-Optical Engineering, National Taiwan University, Taipei, Taiwan, ROC*

[b] *Department of Materials Engineering, Tatung University, Taipei, Taiwan, ROC*

Available online 9 March 2004

Abstract

We report a novel tri-layer bottom antireflective coating (BARC) design based on hexamethyldisiloxane (HMDSO) films working simultaneously at 157, 193 and 248 nm wavelengths. The required optical constant for each layer can be tuned by varying the gas flow rate ratio of oxygen to HMDSO in an electron cyclotron resonance plasma enhanced chemical vapor deposition (ECR-PECVD) process. The swing effect in the resist is experimentally shown to be reduced significantly by adding this tri-layer BARC structure.

1. Introduction

The KrF, ArF and F_2 excimer laser based deep ultraviolet and vacuum ultraviolet lithographies with resolution enhancement techniques are regarded as the main technologies that would lead to the nodes down to 65 nm. The problems of critical dimension (CD) control caused by highly reflective substrates are very serious in these wavelength regimes [1,2]. Therefore, a BARC layer is desirable to overcome problems of CD control.

Conventional spin-coated organic BARC [3] relies on the absorption of reflected light through a relatively thick film. It tends to planarize the topography on a substrate, resulting in varying BARC thickness and thus different reflections from the substrate. As feature size continues to shrink into the sub-micron regime and the stepper projection systems shift to shorter wavelengths, organic BARC cannot easily meet the more stringent substrate and resist requirements. As a result, chemical vapor deposition (CVD) deposited films have been proposed as BARCs for DUV lithographies [2,4]. The CVD-deposited films can provide the possibility of completely eliminating the reflectance from various highly reflective substrates due to the tunability of both composition and thickness. Furthermore, the CVD-deposited BARC has been found to be conformal to topographic substrates, so that CD is easily maintained during pattern transfer [5].

The HMDSO film has been demonstrated as a BARC layer in the form of either single layer or

* Corresponding author. Fax: +886-2-2365-6327.
E-mail address: lon@ntu.edu.tw (L.A. Wang).

0167-9317/$ - see front matter
doi:10.1016/j.mee.2004.02.016

multilayer in the DUV regime [6,7]. The vaporized liquid HMDSO is used as coating material in a conventional ECR-PECVD process. The suitable optical constants of HMDSO films for BARC layers can be tuned through adjusting the gas flow rate ratio of oxygen to HMDSO during deposition.

Here, we report a new HMDSO tri-layer BARC structure design that can work at 248, 193 and 157 nm wavelengths simultaneously.

2. Simulation

Fig. 1 shows the schematic diagram of our tri-layer BARC structure. Layers 1, 2 and 3 are deposited with different gas flow rate ratios of oxygen to HMDSO, and therefore result in HMDSO films with different optical constants [8]. In the multi-layer BARC structure, the extinction coefficient of each layer is gradually increased layer by layer, and is highest at the bottom layer. The combination of the multilayer thin film stack creates a gradual change of optical constants to minimize the reflectance at each BARC layer interface. The light reflected from the highly reflective substrate can be absorbed layer by layer. Thus, the graded-absorption multiplayer structure can be used as BARC layer for highly reflective substrates.

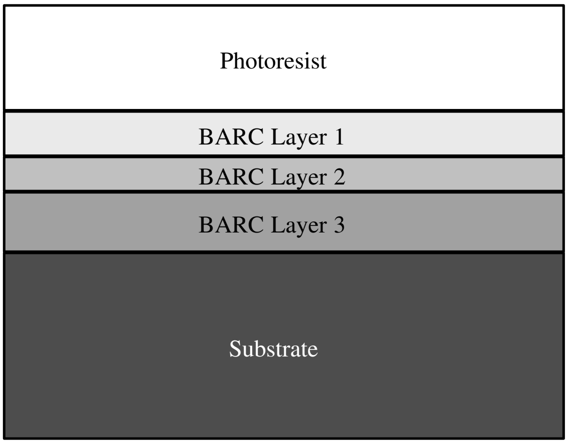

Fig. 1. Schematic diagram of a tri-layer BARC structure.

To find the optimum structure of a BARC layer, we first simulate the characteristics. The reflectance of the film stacks can be calculated by using the characteristic matrix method [9]. Assume a beam is normally incident on a uniform and isotropic thin film, the reflectance R can be expressed as

$$R = \left(\frac{N_0B - C}{N_0B + C}\right)\left(\frac{N_0B - C}{N_0B + C}\right)^* \tag{1}$$

$$\begin{bmatrix} B \\ C \end{bmatrix} = \left(\prod_{r=1}^{3}\begin{bmatrix} \cos\delta_r & (\mathrm{i}\sin\delta_r)/N_r \\ \mathrm{i}N_r\sin\delta_r & \cos\delta_r \end{bmatrix}\right)\begin{bmatrix} 1 \\ N_{sub} \end{bmatrix}, \tag{2}$$

where $N_r = n_r - \mathrm{i}k_r$, and n_r, k_r are optical constants of each film stack; δ_r is the optical phase thickness equal to $2\pi N_r d_r/\lambda$ with d_r as physical film thickness and λ (248, 193 or 157 nm) as exposure wavelength.

The swing effect is caused by optical interference between the fields reflected from air/resist and resist/substrate interfaces. This effect leads to the variation of exposure dosage, and thus induces the CD control issue in the optical lithography process. A CVD-deposited BARC can have constant thickness over the topography of a substrate, but the resist film may have various thicknesses, leading to the swing curve effect.

A simple model of resist reflectance swing ratio, S, can be expressed as follows [3]

$$S \cong 4\sqrt{R_1R_2}\,\mathrm{e}^{-\alpha D}, \tag{3}$$

Table 1
Optical constants of the HMDSO film

Wavelength (nm)	Optical constants					
	Layer 1		Layer 2		Layer 3	
	n_r	k_r	n_r	k_r	n_r	k_r
248	1.484	0.020	1.798	0.103	1.962	0.227
193	1.552	0.015	1.970	0.405	1.971	0.405
157	1.653	0.032	1.924	0.359	1.926	0.619

where R_1 is the reflectance at the resist/air interface; R_2 is the reflectance at the resist/substrate or resist/BARC interface depending on the existence of the BARC layer; α is the absorption coefficient of the resist and D is the thickness of the resist. Therefore, it is very important to reduce R_2 when a BARC structure is introduced. Table 1 shows the optical constants of the HMDSO film employed in the tri-layer structure. The resists used were TER-1 (Microlithography Chemical Corp.) for 193 nm and K30G (JSR) for 248 and 157 nm. According to the simulation results, the optimal thickness of layer 1 is 18 nm, layer 2 is 4 nm, and layer 3 is 70 nm.

3. Experiment setup

The HMDSO films were deposited by employing an ECR-PECVD. The feed gases were HMDSO, O_2 and Ar and the chamber pressure was 2.2×10^{-4} Torr. The ECR microwave power was set to 700 W, the DC bias was fixed at 800V during the deposition, and the substrate was not heated.

The reflectance spectra were measured by using an optical spectrometer (HITACHI, U3501) for 193 and 248 nm wavelengths, and by using a home-made reflective type optical spectrometer with H_2 lamp as excitation source for 157 nm wavelength.

4. Results and discussion

First, a tri-layer AR coating on Si substrate for 248, 193 and 157 nm was simulated and fabricated. To find the optimum structure of the tri-layer AR coating, the reflectance contour at the interface between air and AR coating was calculated first for various thicknesses of layer 1, layer 2 and layer 3 on a Si substrate. Fig. 2 shows the measured and simulated reflectance spectrum from a Si substrate coated with the tri-layer HMDSO films. The measured reflectance was 2.4% at 248 nm and 3.9% at 193 nm.

Figs. 3 and 4 show the measured (triangle dot) and simulated reflectance swing curves of the resists coated on silicon substrates with (solid line) and without (dashed line) BARC at 193 and 248 nm wavelengths, respectively. For 248 nm, the reflectance varies from about 5% to 50% for resist thickness ranging from 550 to 850 nm before adding the BARC layer; then the variation is reduced to about 5–10.5% when the BARC is added. For 193 nm, the reflectance varies from about 1% to 30% for the resist thickness ranging from 300 to 600 nm before adding the BARC layer. The variation is reduced to about 3–10.5% when the BARC is added. Fig. 5(a) shows the simulated reflectance

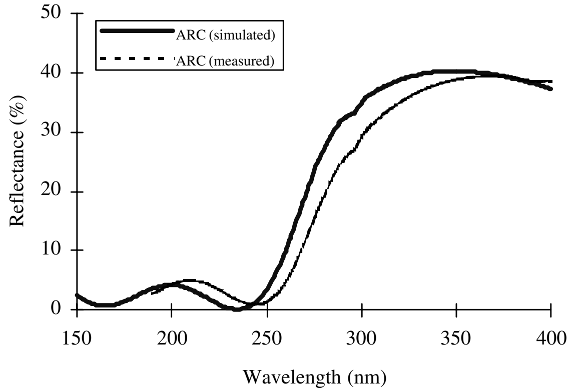

Fig. 2. Simulated and measured reflectance spectrum from a Si substrate coated with the tri-layer HMDSO films. The measured reflectance was 2.4% at 248 nm and 3.9% at 193 nm.

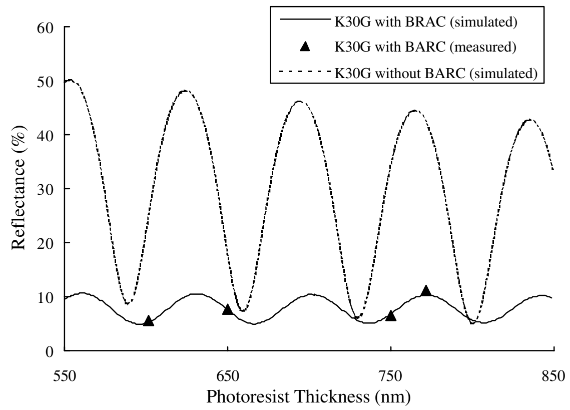

Fig. 3. Reflectance swing curves of resist coated on a silicon substrate before and after the deposition of the tri-layer BARC for 248 nm.

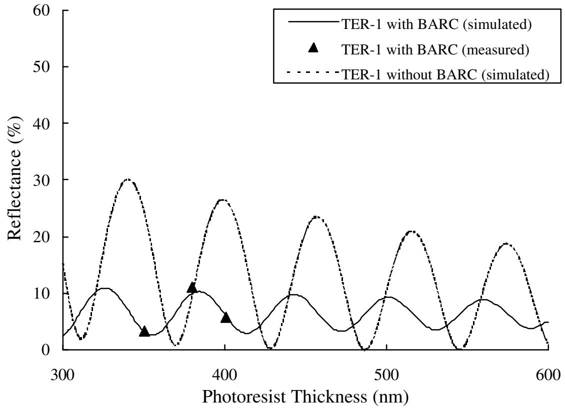

Fig. 4. Reflectance swing curves of resist coated on a silicon substrate before and after the deposition of the tri-layer BARC for 193 nm.

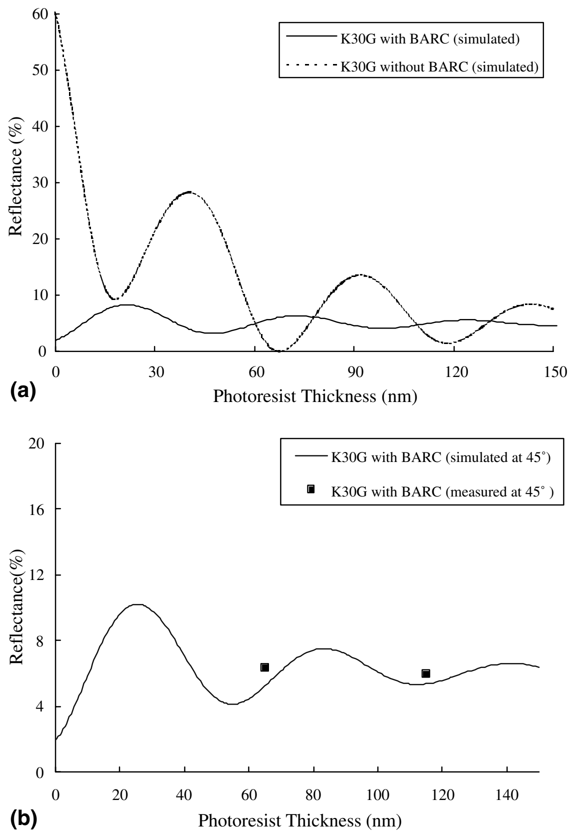

Fig. 5. (a) Simulated reflectance swing curves of resist coated on a silicon substrate before and after the deposition of the tri-layer BARC for 157 nm. (b) Measured (square dots) and simulated reflectance swing curves of the resists coated on silicon substrates with BARC for 157 nm at 45° incidence.

swing curves of the resists coated on silicon substrates with (solid line) and without (dashed line) BARC at 157 nm wavelengths, the reflectance exhibits a variation from about 1% to 60% for the resist thickness ranging from 0 to 150 nm before adding the BARC layer. The variation is reduced to about 2–7.5% when the tri-layer BARC is added. Fig. 5(b) shows the measured (square dots) by using a home-made reflective type optical spectrometer and simulated reflectance swing curves of the resists coated on silicon substrates with (solid line) BARC at 157 nm wavelengths.

The results indicate that the use of such an HMDSO based tri-layer BARC can significantly reduce the swing effects occurred in the resist for 248, 193 and 157 nm wavelengths simultaneously. Therefore, CD control is expected to be greatly improved.

5. Conclusion

The tri-layer film design based on HMDSO is expected to be an effective BARC structure for KrF, ArF and F_2 lithographies simultaneously. The swing effects are shown to be reduced significantly after the BARC layer is added.

References

[1] Y. Sato, E. Shiobara, S. Miyoshi, M. Asano, H. Matsuyama, Y. Onishi, J. Vac. Sci. Technol. B 17 (1999) 3398.
[2] R.A. Cirelli, G.R. Weber, A. Kornblit, R.M. Baker, F.P. Klemens, J. DeMarco, C.S. Pai, J. Vac. Sci. Technol. B 14 (1996) 4229.
[3] R.R. Dammel, R.A. Norwood, Proc. SPIE 2724 (1996) 754.
[4] M. Xu, T.-M. Ko, J. Vac. Sci. Technol. B 18 (2000) 127.
[5] M. Op de Beeck, G. Vandenberghe, P. Jaenen, F.H. Zhang, C. Delvaux, I.V. Puyenbroeck, K. Ronse, Microlithogr. World 7 (1998) 13.
[6] H.L. Chen, L.A. Wang, Appl. Opt. 38 (1999) 4885.
[7] C.H. Lin, L.A. Wang, H.L. Chen, J. Vac. Sci. Technol. B 18 (2000) 3323.
[8] L.A. Wang, H.L. Chen, J. Vac. Sci. Technol. B 17 (6) (1999) 2772.
[9] H.A. Macleod, Thin Film Optical Filters, Macmillan, New York, 1986.